Electron Momentum Spectroscopy Study of Lone Pair Orbitals of Thiols and Dimethyl Sulfide

Masahiko Takahashi, Hikaru Nagasaka, and Yasuo Udagawa*

Research Institute for Scientific Measurements, Tohoku University, Sendai 980-77, Japan

Received: June 27, 1996; In Final Form: September 18, 1996[⊗]

Experimental momentum profiles of the lone pair orbitals of several thiols and dimethyl sulfide have been measured and compared with theoretical momentum profiles. All the observed profiles exhibit p-type character, confirming that the orbitals have been characterized as sulfur nonbonding orbitals. However, small shifts in the profiles are found, depending on substituents. The results are discussed in relation to the geometries of the molecules.

I. Introduction

The molecular orbital approximation of the many-electron wave function is very useful for understanding molecular structures and chemical reactivities in terms of orbital energies and electron distributions. Although orbital energies can be obtained experimentally by photoelectron spectroscopy, it is difficult to determine the orbital character and to obtain the electron distributions.

Electron momentum spectroscopy (EMS) is a unique tool for investigating electron distributions of individual molecular orbitals in momentum space.[1−4] EMS provides more specific information than Compton scattering,[5] which probes the total electronic momentum distribution. Since the familiar position space wave function can be Fourier transformed to give the momentum space wave function, EMS allows us to understand the nature of selected molecular orbitals and can be used as a stringent experimental test of theoretical many-electron wave functions.

Delocalization of lone pair orbitals by methyl substitution has been reported with EMS on NH_3[6−10] and H_2O.[11−14] In the present study, alkyl substituent effects on sulfur nonbonding orbitals are studied with EMS. Experimental momentum profiles (XMPs) of the highest occupied molecular orbitals (HOMOs) of H_2S, C_2H_5SH, *n*-C_3H_7SH, *i*-C_3H_7SH, and $(CH_3)_2S$ have been measured and compared with theoretical momentum profiles (TMPs). Substituent effects on the HOMOs are examined in terms of delocalization with the aid of contour maps in position and momentum spaces.

II. Experimental and Theoretical Methods

A. Experimental Method. Binding energy spectra and momentum distributions were obtained using a symmetric noncoplanar electron momentum spectrometer that is schematically shown in Figure 1. It consists of a spherical electrostatic analyzer and 10 electron detectors and is similar to the one reported by Moore and co-workers.[15,16]

An incident electron beam is produced with a homemade electron gun consisting of a tungsten filament, an electrostatic lens, and two sets of electrostatic deflection plates. The electrons intersect target molecules in a gas cell at the entrance focus of the analyzer. The target gas is introduced through a copper needle of 0.2 mm i.d., the end of which is 2 mm from the focus. The unscattered beam is collected by a Faraday cup and monitored during measurements. A typical beam current was 1 μA. Electrons leaving the scattering point at the polar angle of 45° and azimuthal angles of 0, 13, 26, 37, 49, 173, 188, 202, 217, and 231° pass through decelerating electrostatic lenses and enter the spherical analyzer.

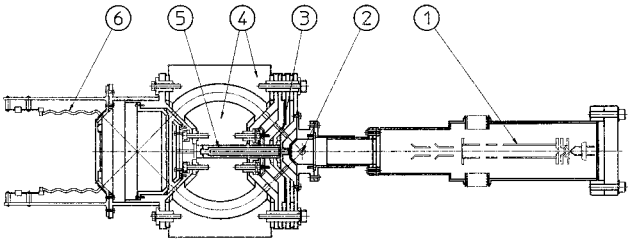

Figure 1. Schematic drawing of the spectrometer used in this work: (1) electron source; (2) entrance focus; (3) deceleration lens; (4) spherical analyzer; (5) Faraday cup; (6) electron multipliers.

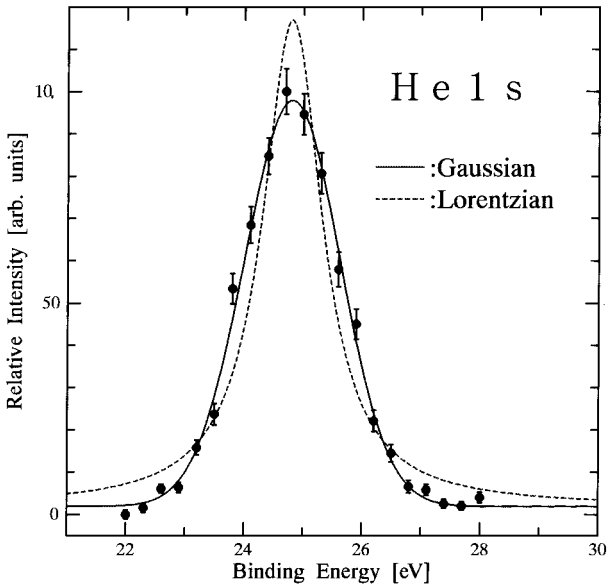

Figure 2. Binding energy spectrum for He 1s ionization. Also shown are the best fit curves assuming a Lorentzian and a Gaussian.

The design of the analyzer is based on the study by Purcell,[17] and the parameters are chosen symmetrically for ease of construction. The angle of deflection is 90°, and the radii of the inner and outer spherical surfaces are 64 and 86 mm, respectively. Herzog plates[18] are employed to compensate for edge effects. Electrons passing through an exit aperture of the analyzer are detected by an array of 10 channel electron multipliers (Murata, Ceratron).

The spectrometer is placed in a vacuum chamber that is evacuated by a 1500 L/s turbomolecular pump to the base pressure of 1×10^{-7} Torr. The electron gun and the detectors

* To whom correspondence should be sent. E-mail: yasuo@vix0.rism.tohoku.ac.jp.

[⊗] Abstract published in *Advance ACS Abstracts,* December 15, 1996.

S1089-5639(96)01912-3 CCC: $14.00

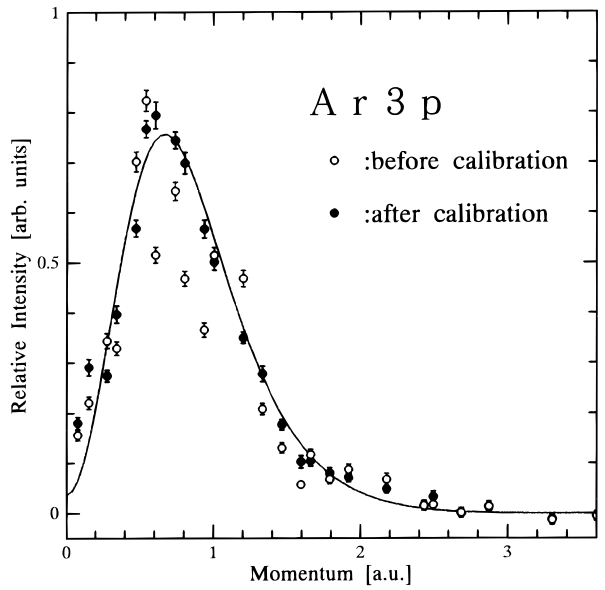

Figure 3. Experimental momentum profiles of Ar 3p before (open circles) and after (solid circles) the calibration. The solid line represents the theoretical momentum profile.

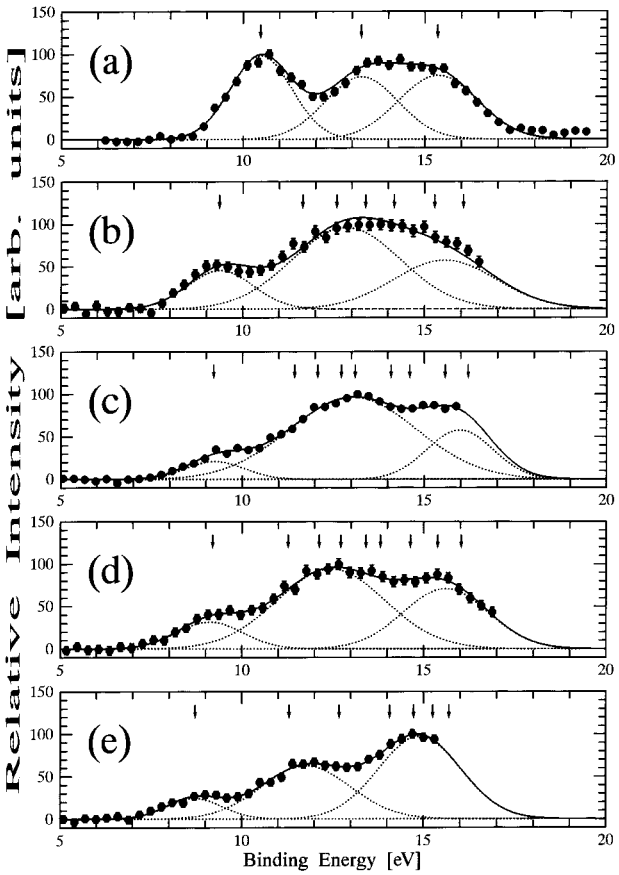

Figure 4. Binding energy spectra of (a) H_2S, (b) C_2H_5SH, (c) *n*-C_3H_7-SH, (d) *i*-C_3H_7SH, and (e) $(CH_3)_2S$. Arrows indicate binding energy levels by HeI photoelectron spectroscopy.

are differentially pumped with 300 L/s turbomolecular pumps to minimize deterioration by reactive gases. By the use of double μ-metal shields, the magnetic field at the spectrometer is below 3 mG.

The pulses from the electron detectors are amplified, discriminated, and converted to ECL logic pulses with a fast monolithic integrated circuit (LeCroy, MVL100). The detectors are divided into groups of five: five located at azimuthal angles less than 50° and the others above 170°. Since the azimuthal angle differences between pairs within the same group correspond to very large momenta, only coincident signals from a detector pair from a different group are selected. Thus, there are 25 such pairs. A circuit that detects coincident events and identifies the detector pair involved has been described in detail by Goruganthu et al.[16] A similar circuit was designed and combined with a computer (NEC, PC9801FA) through a time-to-amplitude converter (ORTEC 566). A typical timing resolution of 10 ns is obtained.

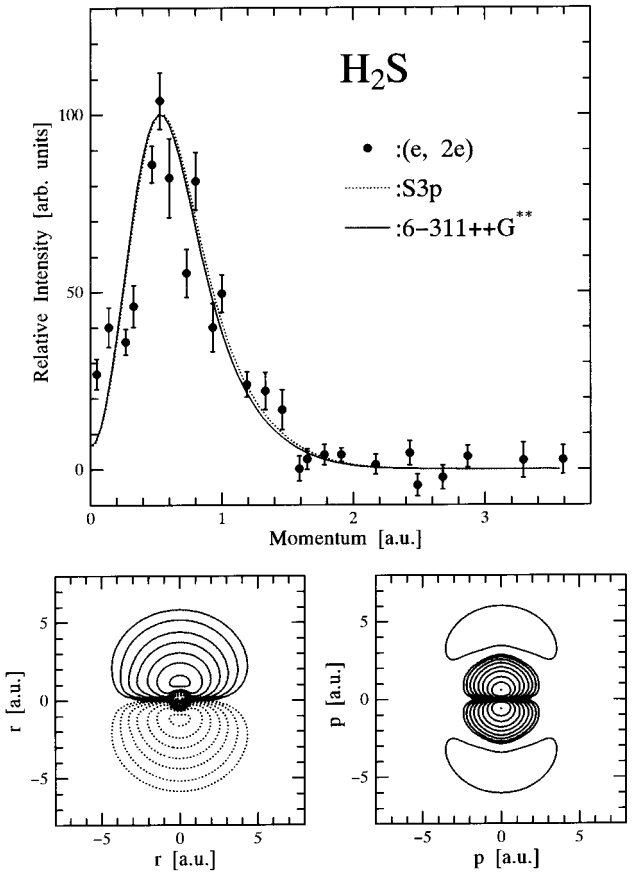

Figure 5. Experimental and theoretical momentum profiles of the HOMO of H_2S. The lower panels show position and momentum space contour maps.

The outgoing electrons were detected at $E = 400$ eV throughout the present experiments. Since the deceleration ratio of the electrostatic lens system was 1/4, the pass energy of the analyzer was set to 100 eV. Binding energy spectra were measured by recording total coincidence counts as a function of the electron gun cathode potential (binding energy $E_b + 800$ eV). A binding energy spectrum for He 1s orbital is shown in Figure 2 to indicate that the band shape is well reproduced by a Gaussian with fwhm of 1.8 eV.

An XMP of a given orbital is obtained from the angular dependence of the coincident counts at an appropriately chosen E_b. However, since the next HOMO overlaps to some extent, deconvolution procedures were employed to construct XMPs of HOMOs. Under the present experimental conditions a momentum range from 0.1 to 3.6 au can be covered. In multichannel spectrometers it is necessary to make calibrations because transmission efficiency and sensitivity of detectors may vary. In the present experiment accidental coincidence count rates were used to calibrate efficiencies of detector pairs. Figure 3 shows XMPs of Ar 3p before and after the calibration and compares them with a TMP. In the calculation the Hartree−Fock quality wave function of Clementi and Roetti[19] was used and the profile was obtained by a convolution assuming a momentum resolution of 0.1 au. It is evident that the calibration procedure employed here reproduces the TMP quite well.

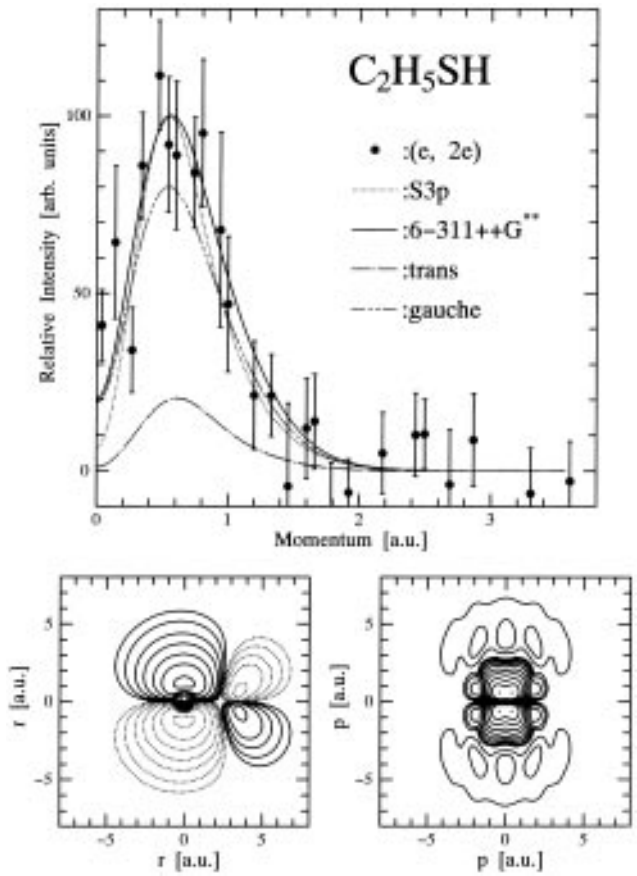

Figure 6. Experimental and averaged theoretical momentum profiles of the HOMO of C_2H_5SH. The contributions of each conformer to the TMP are also indicated. The lower panels show position and momentum space contour maps for a *trans*-C_2H_5SH molecule.

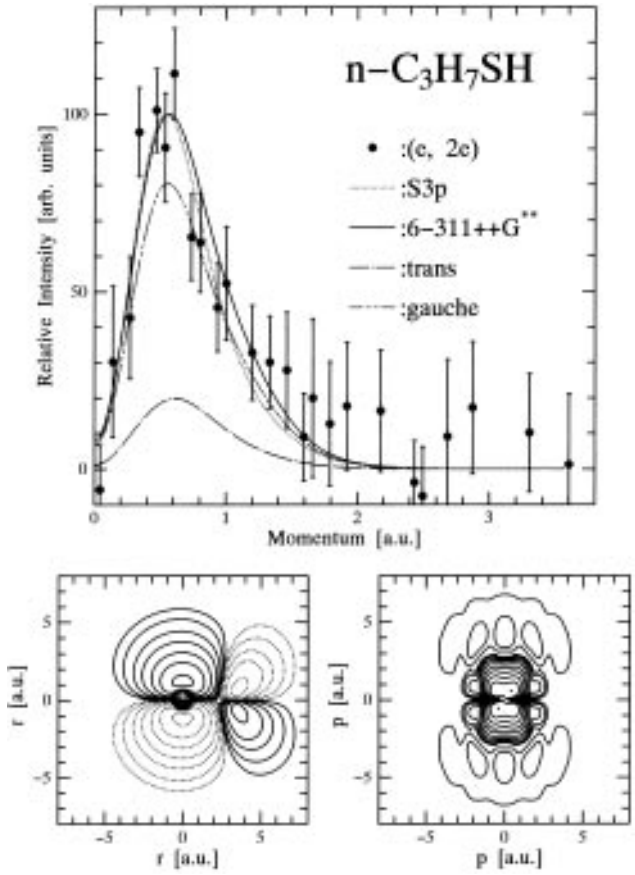

Figure 7. Experimental and averaged theoretical momentum profiles of the HOMO of *n*-C_3H_7SH. The contributions of each conformer to the TMP are also indicated. The lower panels show position and momentum space contour maps for a *trans*-*n*-C_3H_7SH molecule.

TABLE 1: Summary of the Peak Maxima in the Electron Momentum Distributions

	p_{max}[a]		
	trans	*gauche*	average
H_2S	0.52		0.52
CH_3SH	0.61		0.61
C_2H_5SH	0.61	0.54	0.56
n-C_3H_7SH	0.61	0.54	0.56
i-C_3H_7SH	0.46	0.53	0.51
$(CH_3)_2S$	0.68		0.68

[a] In au.

High-purity H_2S gas (>99.9%) was obtained from Nippon Sanso and used without further purification. C_2H_5SH, *n*-C_3H_7SH, *i*-C_3H_7SH, and $(CH_3)_2S$ (Wako and Tokyo Kasei) were subjected to repeated freeze−pump−thaw cycles before use. It took 3−4 weeks to accumulate sufficient data for each molecule.

B. Theoretical Calculations. Theoretical calculations of the wave functions in position space were carried out by Gaussian 92 at Computing Center of Institute for Molecular Science. Geometries of the molecules studied here, H_2S,[20,21] CH_3SH,[22−26] C_2H_5SH,[27,28] and $(CH_3)_2S$,[29] were taken from the literature. Geometries of *n*-C_3H_7SH and *i*-C_3H_7SH were optimized by the use of the 6-311G** basis set, fixing a part of the structural parameters[30,31] determined by microwave spectroscopy. Then theoretical wave functions of all the molecules were calculated using the 6-311++G** basis set. Diffuse functions are included for all atoms, which is expected to improve descriptions of lone pair orbitals.

It has been known that two conformers exist for several molecules studied here: *trans* and *gauche* for C_2H_5SH and *i*-C_3H_7SH and *trans*−*trans* and *gauche*−*trans* (hereafter called *trans* and *gauche*, respectively) for *n*-C_3H_7SH, where the first refers to the isomerism around C−S bond and the second to that around the central C−C bond. The *gauche* form is more stable by 142 and 136 cm^{-1} for C_2H_5SH[32] and *n*-C_3H_7SH,[30] respectively, while the *trans* form is more stable by 20 cm^{-1} for *i*-C_3H_7SH.[31] Accordingly, population ratios of the *trans* and *gauche* forms at room temperature are ca. 1:4, 1:4, and 1:2 for C_2H_5SH, *n*-C_3H_7SH, and *i*-C_3H_7SH.

Calculations of spherically averaged momentum distributions from the wave functions in position space were carried out using a program supplied by Brion and co-workers and then convoluted with the instrumental resolution of 0.1 au. Averaged TMPs were also calculated for molecules having isomers to make comparison with XMPs.

III. Results

The binding energy spectra of all the molecules studied here are shown in Figure 4. Each spectrum is the sum of the signals from the 25 detector pairs. Also indicated by arrows are binding energy levels by He I photoelectron spectroscopy.[33] Although lower energy levels are rather densely spaced, binding energies of HOMOs are separated from the next HOMO by at least 2.0 eV. Thus, it is possible to subtract contributions from overlapping MO's by deconvolution procedures assuming a Gaussian with fwhm of 1.8 eV. Deconvoluted curves are also given in the figure.

Figures 5−9 show XMPs of the HOMOs of H_2S, C_2H_5SH, *n*-C_3H_7SH, *i*-C_3H_7SH, and $(CH_3)_2S$, together with the TMPs using the 6-311++G** basis set. The TMP of the sulfur 3p atomic orbital, which also serves as a measure of comparison of the differences in XMPs of the molecules studied, is shown in each figure. All XMPs exhibit p-type character; the intensity

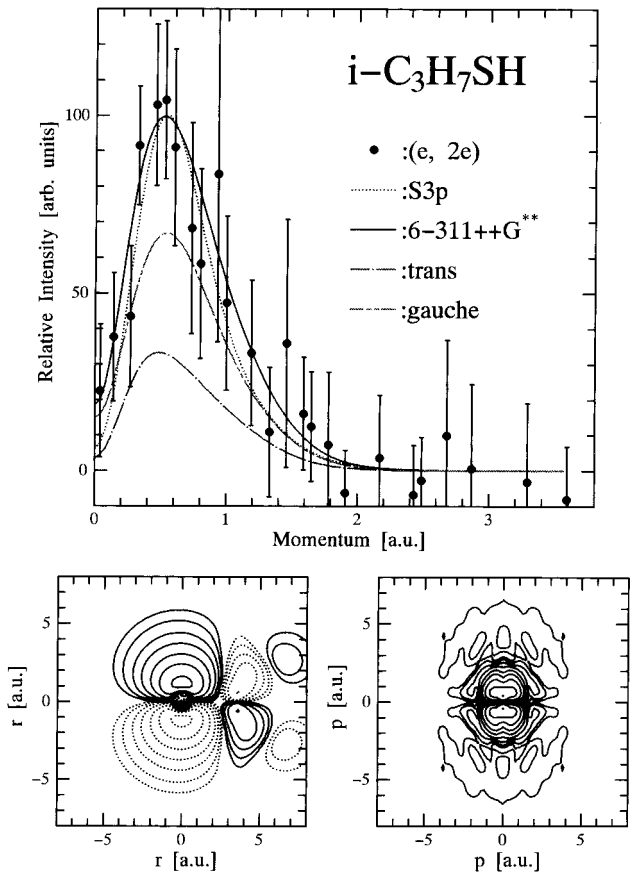

Figure 8. Experimental and averaged theoretical momentum profiles of the HOMO of *i*-C_3H_7SH. The contributions of each conformer to the TMP are also indicated. The lower panels show position and momentum space contour maps for a *trans*-*i*-C_3H_7SH molecule.

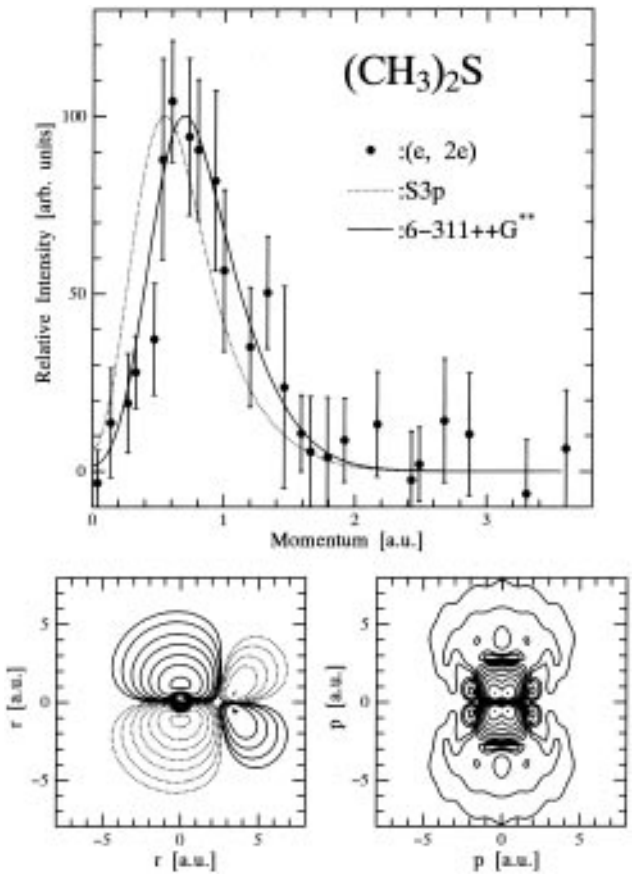

Figure 9. Experimental and theoretical momentum profiles of the HOMO of $(CH_3)_2S$. The lower panels show position and momentum space contour maps.

almost vanishes near the origin and has a single maximum. It agrees with the previous assignments that all the HOMOs have been characterized as sulfur nonbonding orbitals. TMPs using the 6-311++G** basis set reproduce the XMPs within experimental uncertainties.

Position and momentum space density contour maps of the HOMOs are shown in the bottom panels of Figures 5−9. These maps are slices of the electron density in position and momentum spaces through the plane of S and C backbones of each molecule (S and H in Figure 5) oriented such that the H−S−C plane is perpendicular to the vertical axis (C−S−C in Figure 9). In the position space maps the S atom is placed at the origin. The contour values represent 0.01, 0.03, 0.1, 0.3, 1.0, 3.0, 10.0, 30.0, and 99.0% of the maximum density.

IV. Discussion

An EMS study of the HOMO of H_2S has already been reported by French et al.[34] They observed that it is essentially an atomic-like 3p orbital on sulfur. The TMP using the 6-311++G** basis set almost overlaps with that of the sulfur 3p atomic orbital as is shown in Figure 5. Atomic orbital-like nature is evident in both the position and the momentum space density maps. In the former electron density is localized on the S atom, and in the latter there is no indication of bond formation that should manifest itself in "wrinkles" due to the interference effects.[35,36]

On the other hand, position space maps, momentum space maps, and momentum profiles all demonstrate that HOMOs of the thiols and dimethyl sulfide are molecular in nature. The position space maps indicate some density on the neighboring C atom and show that there always is a node between the S and C atoms. Although not apparent in the figure, an examination of atomic orbital (AO) coefficients indicates that contributions to the HOMO from AOs of other atoms are not significant. An exception is *trans*-*i*-C_3H_7SH, which will be discussed in detail later.

Delocalization of the HOMOs of thiols and dimethyl sulfide is evident also in momentum space maps that show "wrinkled" contours. It reflects the interference effects, usually called bond oscillations,[35,36] due to multiple atomic centers participating in the bonding or antibonding interaction. An increase in the number of nodal surfaces in position space and the resultant bond oscillations in momentum space contribute to an increase in high momentum components of the momentum distributions.[8,10,11,13,37−39] Thus, it accounts for the observation that TMPs of thiols and dimethyl sulfide, except for *trans*-*i*-C_3H_7SH, shift to higher momentum compared with that of H_2S. Calculated p_{max} values are summarized in Table 1. The shift of p_{max} of dimethyl sulfide is much more than that of thiols because there are two nodes in dimethyl sulfide between S and the two equivalent C atoms.

A similar tendency has been found in the earlier EMS studies of the HOMOs of H_2O[12] and CH_3OH.[11] The p_{max} values are estimated to be ∼0.6 and ∼0.9 au from the literature. Table 1 shows that shifts of p_{max} values of thiols are much less than that of methanol. Thus, the antibonding interaction between the S and neighboring C atoms is much weaker. Further alkylation of the carbon adjacent to S has little effect on the S lone pair orbital. An exception is *trans*-*i*-C_3H_7SH, which has a very small p_{max} value.

In addition to the methyl substituent effects described above, it has also been reported that increasing methylation leads to increasing cross section at low momentum in the HOMOs of CH_3OH and $(CH_3)_2O$. In particular, Clark et al.[13] observed that XMP of HOMO of $(CH_3)_2O$ is very broad and has a consider-

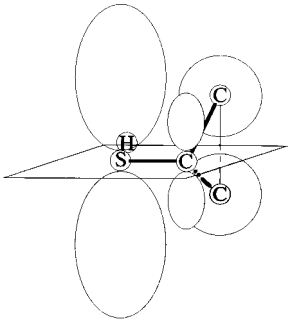

Figure 10. Schematic atomic orbital representation of the HOMO of *trans-i*-C_3H_7SH.

able intensity near the origin. They interpreted the phenomenon in terms of the delocalization of the HOMO to H atoms of the methyl groups. In $(CH_3)_2O$ two pairs of hydrogen atoms happen to lie symmetrically above and below the O−C−O plane, making a combination of two s functions a pseudo p function. Hence, in addition to p functions centered on the O and C atoms, the pseudo p functions make a significant contribution to the HOMO. In-plane H atoms make no contribution.

Since no significant increase in low momentum components was observed in the XMPs and associated TMPs of thiols and dimethyl sulfide, delocalization of HOMOs of these molecules is concluded to be less extensive. As mentioned previously, however, *trans-i*-C_3H_7SH shows an exceptionally low p_{max} value in the TMP.

An examination of the position space wave function reveals that an effect similar to the one observed for $(CH_3)_2O$ makes *trans-i*-C_3H_7SH exceptional. Figure 10 shows that in *trans-i*-C_3H_7SH two C−C bonds stick out above and below the H−S−C plane**.** As a result, 2s orbitals of the two C atoms, like a pair of 1s orbitals of H in $(CH_3)_2O$, make a pseudo p orbital and participate in the HOMO. Since the amplitude is in-phase with that of the S nonbonding orbital, it contributes to increased low momentum components of the momentum distribution.[37] Unfortunately, this effect was not observed in the XMP, since *trans-i*-C_3H_7SH is a minor component at room temperature.

In summary, an EMS study indicates that the HOMOs of the molecules studied here are more "pure" lone pair orbitals than the corresponding oxygen compounds. Furthermore, the weak substituent effects on the TMPs indicate that the antibonding interaction between the S and neighboring C atom(s) mainly determines the nature of the HOMOs. Further alkylation of the carbon adjacent to S makes little change in the orbital character. An exception is *trans-i*-C_3H_7SH in which, owing to its geometrical structure, 2s orbitals of the second nearest-neighbor C atoms also participate in the HOMO.

Acknowledgment. We thank Mr. H. Yoshida and Mr. H. Watanabe at the Institute for Molecular Science for help in developing the electronics of the present apparatus and for the advice to carry out theoretical calculations, respectively. We are indebted to all the staff of the machine shop at our institute for their help with the design and construction of the apparatus. We are also indebted to Professor Brion, Dr. J. J. Neville, and Dr. N. Cann at The University of British Columbia for providing a program to calculate spherically averaged momentum distributions. This work is partly supported by a Grant-in-Aid for Scientific Research No. 07404032 from the Ministry of Education, Science and Culture.

References and Notes

(1) McCarthy, I. E.; Weigold, E. *Phys. Rep.* **1976**, *C27*, 275.
(2) Brion, C. E. *Int. J. Quantum Chem.* **1986**, *XXIX*, 1397.
(3) Weigold, E. *Z. Naturforscher* **1993**, *48A*, 371.
(4) Coplan, M. A.; Moore, J. H.; Doering, J. P. *Rev. Mod. Phys.* **1994**, *66*, 985.
(5) *Compton Scattering*; Williams, B., Ed.; McGraw-Hill: London, 1977.
(6) Tossell, J. A.; Lederman, S. M.; Moore, J. H.; Coplan, M. A.; Chornay, D. J. *J. Am. Chem. Soc.* **1984**, *106*, 976.
(7) Rosi, M.; Cambi, R.; Fantoni, R.; Tiribelli, R.; Bottomei, M.; Giardini-Guidoni, A. *Chem. Phys.* **1987**, *116*, 399.
(8) Bawagan, A. O.; Brion, C. E. *Chem. Phys. Lett.* **1987**, *137*, 573.
(9) Bawagan, A. O.; Muller-Fiedler, R.; Brion, C. E.; Davidson, E. R.; Feller, D. *Chem. Phys.* **1988**, *120*, 335.
(10) Bawagan, A. O.; Brion, C. E. *Chem. Phys.* **1988**, *123*, 51.
(11) Minchinton, A.; Brion, C. E.; Weigold, E. *Chem. Phys.* **1981**, *62*, 369.
(12) Bawagan, A. O.; Brion, C. E.; Davidson, E. R.; Feller, D. *Chem. Phys.* **1987**, *113*, 19.
(13) Clark, S. A. C.; Bawagan, A. O.; Brion, C. E. *Chem. Phys.* **1989**, *137*, 407.
(14) Zheng, Y.; Weigold, E.; Brion, C. E.; von Niessen, W. *J. Electron Spectrosc. Relat. Phenom.* **1990**, *53*, 153.
(15) Moore, J. H.; Coplan, M. A.; Skillman, T. L.; Brooks, E. D., III. *Rev. Sci. Instrum.* **1978**, *49*, 463.
(16) Goruganthu, R. R.; Coplan, M. A.; Moore, J. H.; Tossell, J. A. *J. Chem. Phys.* **1988**, *89*, 25.
(17) Purcell, E. M. *Phys. Rev.* **1938**, *54*, 818.
(18) Herzog, R. *Z. Phys.* **1935**, *97*, 596.
(19) Clementi E.; Roetti, R. *At. Data Nucl. Data Tables* **1974**, *14*, 177.
(20) Edwards, T. H.; Moncur, N. K.; Snyder, L. E. *J. Chem. Phys.* **1967**, *46*, 2139.
(21) Burrus, C. A.; Gordy, W. *Phys. Rev.* **1953**, *92*, 274.
(22) Kojima, T.; Nishikawa, T. *J. Phys. Soc. Jpn.* **1957**, *12*, 680.
(23) Kilb, R. W. *J. Chem. Phys.* **1955**, *23*, 1736L.
(24) Solimene, N.; Dailey, B. P. *J. Chem. Phys.* **1955**, *23*, 124.
(25) Solimene, N.; Dailey, B. P. *Phys. Rev.* **1953**, *91*, 464A.
(26) Shaw, T. M.; Windle, J. J. *J. Chem. Phys.* **1951**, *19*, 1063L.
(27) Hayashi, M.; Imaishi, H.; Kuwada, K. *Bull. Chem. Soc. Jpn.* **1974**, *47*, 2382.
(28) Nakagawa, J.; Kuwada, K.; Hayashi, M. *Bull. Chem. Soc. Jpn.* **1976**, *49*, 3420.
(29) Iijima, T.; Tsuchiya, S.; Kimura, M. *Bull. Chem. Soc. Jpn.* **1977**, *50*, 2564.
(30) Nakagawa, J.; Hayashi, M. *J. Mol. Spectrosc.* **1981**, *85*, 327.
(31) Griffiths, J. H.; Boggs, J. E. *J. Mol. Spectrosc.* **1975**, *56*, 257.
(32) Schmidt, R. E.; Quade, C. R. *J. Chem. Phys.* **1975**, *62*, 3864.
(33) Kimura, K.; Katsumata, S.; Achiba, Y.; Yamazaki, T.; Iwata, S. *Handbook of HeI Photoelectron Spectra of Fundamental Organic Molecules*; Halsted: New York, 1981.
(34) French, C. L.; Brion, C. E.; Davidson, E. R. *Chem. Phys.* **1988**, *122*, 247.
(35) Leung, K. T.; Brion, C. E. *Chem. Phys.* **1983**, *82*, 113.
(36) Bawagan, A. O.; Lee, L. Y.; Leung, K. T.; Brion, C. E. *Chem. Phys.* **1985**, *99*, 367.
(37) Coulson, C. A. *Proc. Cambridge Philos. Soc.* **1941**, *37*, 74.
(38) Bawagan, A. O.; Brion, C. E.; Coplan, M. A.; Tossell, J. A.; Moore, J. H. *Chem. Phys.* **1986**, *110*, 153.
(39) McMillan, K.; Coplan, M. A.; Moore, J. H.; Tossell, J. A. *J. Phys. Chem.* **1990**, *94*, 8648.